Available online at www.CivileJournal.org

Civil Engineering Journal

Vol. 6, No. 6, June, 2020

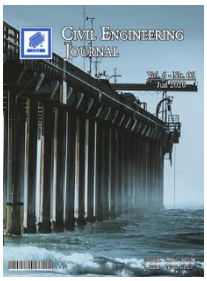

One-Dimensional Hydrodynamic Modeling of the Euphrates River and Prediction of Hydraulic Parameters

Nassrin Jassim Hussien Al-Mansori [a*], Laith Shaker Ashoor Al-Zubaidi [a]

[a] *Department of Environmental Engineering, University of Babylon, Babylon, 00964, Iraq.*

[b] *Ministry of Industry and Minerals, Babylon, 00964, Iraq.*

Received 13 December 2019; Accepted 20 March 2020

Abstract

Forecasting techniques are essential in the planning, design, and management of water resource systems. The numerical model introduced in this study turns governing differential equations into systems of linear or non-linear equations in the flow field, thereby revealing solutions. This one-dimensional hydrodynamic model represents the varied unsteady flow found in natural channels based on the Saint-Venant Equations. The model consists of the equations for the conservation of mass and momentum, which are recognized as very powerful mathematical tools for studying an important class of water resource problems. These problems are characterized by time dependence of flow and cover a wide range of phenomena. The formulations, held up by the four-point implicit finite difference scheme, solve the nonlinear system of equations using the Newton-Raphson iteration method with a modified Gaussian elimination technique. The model is calibrated using data on the Euphrates River during the early spring flood in 2015. It is verified by its application to an ideal canal and to the reach selected at the Euphrates River; this application is also used to predict the effect of hydraulic parameters on the river's flow characteristics. A comparison between model results and field data indicates the feasibility of our technique and the accuracy of results (R^2 = 0.997), meaning that the model is ready for future application whenever field observations are available.

Keywords: Hydrodynamics; River; Surface Water; Numerical Model; Finite Element; Flow.

1. Introduction

Open channels are found in natural rivers, basins and estuaries. Many problems in water resources, river mechanics and environmental hydraulics require accurate descriptions of the flow regime parameters regime in open channels. As a result, the study of the development and management of water resources has become highly relevant for engineers. A mathematical model is a representation of the behavior of a particular system in the form of mathematical equations. By specifying parameters within mathematical models, system responses can be determined. Though they usually function as a design tool, these models may also be used for the real-time control or operation of a system. The following steps are generally involved in the development of mathematical models: derivation of governing equations; selection of solution procedures; and calibration and verification of the model.

Jacob et al. (2019) used a hydrologic-hydraulic approach to assess survey the information rare lower Bharathapuzha basin in Kerala, India. They developed a completely hydrodynamic one-dimensional (1D) waterway stream model is aligned in 1992 and validated in 1994. They then use a coupled 1D-2D flood immersion model to simulate the degree of flooding in 2002. A suitable methodology is used to derive this information from the partially cloud-secured WiFS

* Corresponding author: nassrin20052001@yahoo.com

http://dx.doi.org/10.28991/cej-2020-03091530

picture. Regional flood frequency estimates and the flood inundation model are then used to assess the severity of the flood hazard [1]. Buček et al. (2019) assess the hydro-morphologic evolution of meander cut-offs for three river restoration scenarios during 10 days of bank-full discharge. They simulate hydro-morphologic dynamics using R2DM, a numerical model with a movable bed [2]. Results for scenarios with a partially opened meander indicate aggradation at the inlet of the meander and a ten present reduction in flow rate. Scenarios with a fully opened meander also show aggradation at the inlet as well as a 55 present reduction in flow rate. Full diversion scenarios result in the formation of natural river landforms (point bars, cut banks, pools, riffles) and the stabilization of river bed evolution.

Glubt et al. (2017) used a 2D (longitudinal and vertical) hydrodynamic and water quality model to simulate the Chehalis River, which includes stretches of free-flowing river and, during the summer, stratified lake-like stretches. The goal of this research was to assess the flood retention structure's impact on water quality and river responses to potential climate change scenarios. Flood retention structures (which operate only during times of flooding) gave model predictions for daily maximum temperature higher than structures that employed both flood retention and flow augmentation (which operate year-round) [3]. Sitek et al. (2017) estimated hydrodynamic forces by using advanced, computational fluid dynamics (CFD). They investigated a section of a model rockery comprised of large boulders exposed to a variety of hydraulic flow conditions and, using the CFD model, calculated new terms for a parametric set of geometry and condition variation. Moreover, formulas for dimensionless hydraulic force coefficients were proposed that can be used for designing new model rockeries or evaluating existing dry-stack rockeries in river environments [4].

Brown et al. (2019) developed a model to run various sediment diversion scenarios. The morphologic modelling results of the diversion scenario analysis show net land gain in the near vicinity of diversion outlets and net land loss further from the outlets. This indicates that diversion-induced inundation leads to a reduction in plant productivity, which induces an acceleration of land loss. When operations cease, salinity recovery is almost entirely determined by prevailing offshore and/or riverine conditions [5]. Chen and Liu (2017) presented three algorithms to resample river cross-section data points in both transverse and longitudinal directions from the original data. A 2D, high-resolution, unstructured-grid hydrodynamic model was used to assess the performance of the original model. The researchers resampled cross-section data on a simulated river stage under low-flow and high-flow conditions, Results indicate that the 2D and 3D models produce similar river stages in both tidal and non-tidal river segments under the low-flow condition [6]. Pramanik et al. (2010) used 40 cross sections along the reaches of the Brahmani River basin in eastern India. After extracting data from the Digital Evaluation Model (DEM), researchers used it to form a Mike 11 hydrodynamic model; the calibrated values of Manning's n were found to vary between 0.02 and 0.033. The study revealed that freely available SRTM DEM-extracted river cross-sections could be used in hydraulic models to simulate stage and discharge hydrographs with considerable accuracy despite the scarcity of measured cross-section data [7]. Only a few studies have focused on modelling riverine flooding of Indian basins (Singh 2004 [8]; Vijay et al. 2007 [9]). The variety of space-time flow and water level in the waterway is figured utilizing Saint-Venant equations (Wang et al. 2000 [10]; Gottardi and Venutelli 2004 [11]; Meng et al 2006 [12]). The conditions are appropriate to shallow water flow conditions, which are administered by the laws of protection of mass and force. Unsteady flow conditions in waterways are re-enacted with significant precision by utilizing these conditions.

The joining of Geographic Information Systems (GIS) with the water driven models is the result of recent advances in computational river hydraulics (Dutta et al. 2000 [13]; Renyi and Nan 2002 [14]; Merwade et al. 2008 [15]). A water powered model coupled with GIS uses the DEM to remove stream cross-areas, which define the geometry of rivers. These waterway cross-areas are then utilized in the waterway model to compute water level and flow. Zhu et al. (2014) showcased the development and validation of a 1D stream hydrodynamic model for surface and groundwater communications (RHM-SG). The model approval tests - including uniform stream over inclining bed, one flood procedure and waterway stream with cooperation of groundwater - demonstrate that the model accurately characterises the interaction between river flow and groundwater. The model was applied to the middle reach of the Heihe River, which showed that the accuracy of predicted flow is substantially improved by including surface-groundwater interactions. The correlation coefficient increases from 0.89 to 0.98 and the root-mean-square decreases from 21.16 m^3/s to 8.49 m^3/s [16]. The connection among surface and groundwater is a characteristic wonder; it is particularly critical for shallow wide waterways with sandy bottoms [17]. Akiyama et al. (2007) have recommended that the river water recharges groundwater in lower desert arrives at utilizing stable isotope tracers [18]. Since river stages vary between seasons, the dynamic variations in stream heading between the waterway and groundwater ought to be considered [19, 20].

Mukesh and Narendra (2018) analysed the inundation parameters, established hazard assessment criteria, delineated the extent of flood inundation and identified hazardous areas in different discharge scenarios of 25, 50 and 100 years return period flows. Based on goodness-of-fit tests and fitting parameters, the generalised extreme event (GEV) distribution method is used for flood frequency analysis [21]. The model is calibrated with measured water surface elevation and simulation results. The study concludes that, within the stretch of around 50 km from the Chatara Barrage to the Koshi Barrage, floodwater will not rise above embankments and the left overbank is in the low-

danger zone. The modelling approach proposed in this study is an attractive option for modelling exceptional flood events when limited data and resources are available.

The previous hardly any decades have seen remarkable improvement in the advancement of PC models to recreate floods; much of this was driven by the requirement for devices to assess flood hazard. A large portion of these techniques depend on a nonlinear hyperbolic arrangement of shallow water conditions depicting the preservation of mass and force in two level measurements [22-25].

For this study, due to complex geometry, large flood plains and flow conditions, a 2D hydrodynamic model is required. A 2D hydrodynamic model would capture the effects of the crosscurrents and the complex configuration of the river. There have been several programs developed to simulate 2D flow. Nays 2DH was selected from the available software due to its numerous worldwide applications and, in particular, its applications in fluvial channels. It has the capacity to incorporate complex boundaries and river bed shapes, confluences of main channels and tributaries, bottom friction, vegetation effects and flow fields into its analysis. The main objective of this work is to simulate the flow in the Al-Hindiya barrage reach. This will be done by solving Saint-Venant equations and studying the effects of variation in certain hydraulic parameters (such as distance increment, time increment, and velocity and dispersion coefficient) on hydrodynamic system performance and concentration distribution.

2. Material and Methods

2.1. Unsteady Flow Equations

The unsteady 1D equations of continuity and momentum for gradually varied flow in open channels used in this study are as follows:

$$\frac{\partial Q}{\partial x} + \mathrm{B}\frac{\partial y}{\partial t} \pm q = 0 \tag{1}$$

$$\frac{\partial Q}{\partial t} + \frac{\partial}{\partial x}\left(\frac{Q^2}{\mathrm{A}}\right) \pm q\frac{Q}{\mathrm{A}} = g.\mathrm{A}\left(S_o - S_f - \frac{\partial y}{\partial x}\right) \tag{2}$$

The two equations together comprise an arrangement of nonlinear, hyperbolic incomplete differential conditions in the two questions (Q: release; y: profundity) and two autonomous factors (t: time; x: separation) along the channel reach. The reconciliation of these conditions is cultivated utilizing an understood limited distinction technique.

2.2. Finite Difference Solution

The system of 2N nonlinear equations in 2N unknowns is solved for each time step by the Newton-Raphson method. The computational procedure for each time (j+1) starts by assigning trial values to the 2N unknowns. These trial values of Q and y are those known at time j from the initial conditions or from calculations during the previous time step. The boundary condition equations represent the equations accomplished of the system to be the known number equate the equations number. The external boundary conditions are typically one of the following three types:

- The function y (t) (the stage hydrograph) is known;
- The function Q (t) (the discharge hydrograph) is known;
- The relationship Q = f (y) (the rating curve) is known.

If the stage hydrograph is known, the case is represented mathematically by:

$$G_i\left(y_i^{j+1}, Q_i^{j+1}\right) = y_1^{j+1} - y(t) = 0 \tag{3}$$

With partial derivatives:

$$\frac{\partial G_i}{\partial y_i^{j+1}} = 1 \tag{4}$$

$$\frac{\partial G_i}{\partial Q_i^{j+1}} = \varepsilon \tag{5}$$

Where, G: corresponds to the upstream function. ε: is assigned a very small value, such as 0.0000001, to avoid a zero value for the first matrix coefficient and run the solution algorithm without the otherwise necessary row interchanges.

2.3. Description of the Study Reach

This study considers 550 kilometres of fluvial reach on the Euphrates River from the Al-Hindiya Barrage towards Al-Mahaweel. The location of the study area has shown in Figures 1 and 2.

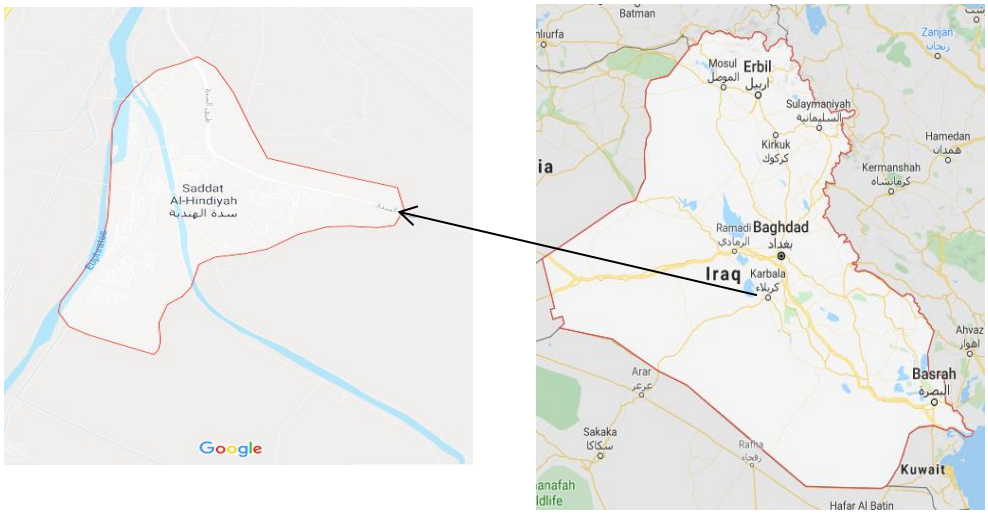

Figure 1. General Layout of the Reach

Figure 2. Exact Location of the Reach, (AL-Hindiya Barrage)

2.4. Channel Geometry

Data on the Euphrates river system typically sees the system divided into small segments; the discretised form of the mathematical model has 20 nodes and 19 reaches. Distance between the nodes and the initial boundary is listed in Table 1. Figure 3 shows a flowchart of the research methodology.

Table 1. Initial Conditions and Distance Increment of the Reach on 1/4/2017

Section No.	Depth m	Discharge m^3/s	Distance interval Km
1	4.423	166.9	0.00
2	4.419	166.5	0.200
3	4.409	166.2	0.450
4	4.395	165.9	0.458
5	4.361	165.7	0.490
6	4.295	165.5	0.500
7	4.263	165.3	0.530
8	4.23	165	0.560
9	4.21	165	0.600
10	4.168	164.7	0.650
11	4.136	164.7	0.700
12	4.088	164.6	0.850
13	4.035	164.5	0.900
14	4.015	164.5	1.060
15	4.014	164.4	1.100
16	4. 120	164.4	1.200
17	4.090	164.2	1.250
18	4.080	164.1	1.300
19	4.050	164.0	1.450
20	4.000	164.0	1.550

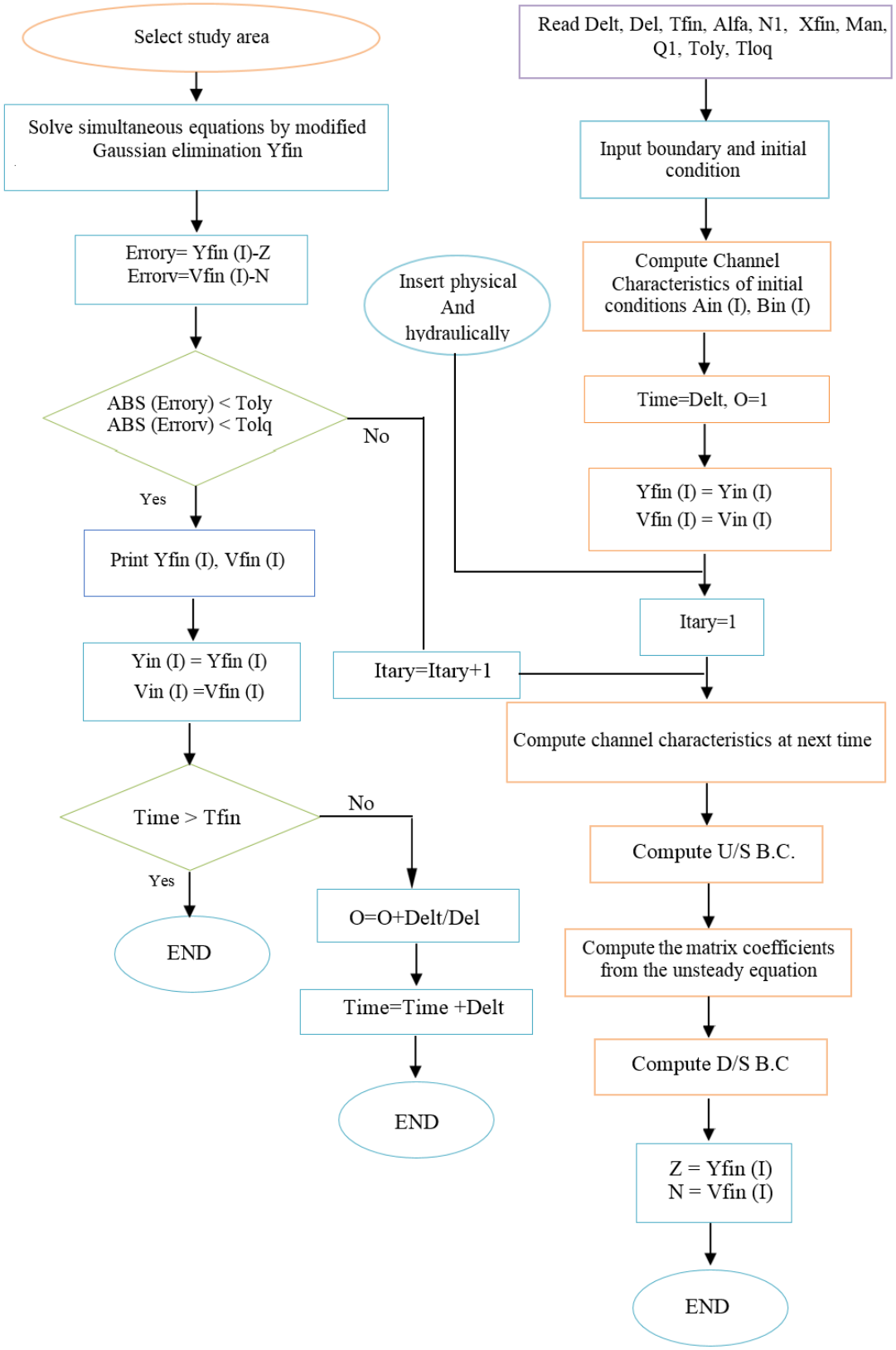

Figure 3. Flowchart of research methodology

To apply this model to the Euphrates River, relevant data is necessary. The channel sections considered in this study are generally irregular; they vary from parabolic to trapezoidal shape approximation. Some of the sections are as deep as a valley while others are shallow. Therefore, the change in flow depth lead to change cross section, top width and wetted perimeter. These parameters may be classified in tabulated values or functional relationships, depending on flow depth. The information required in the HEC-RAS program is displayed on the cross-profile of the river with data editor as shown in Figure 4.

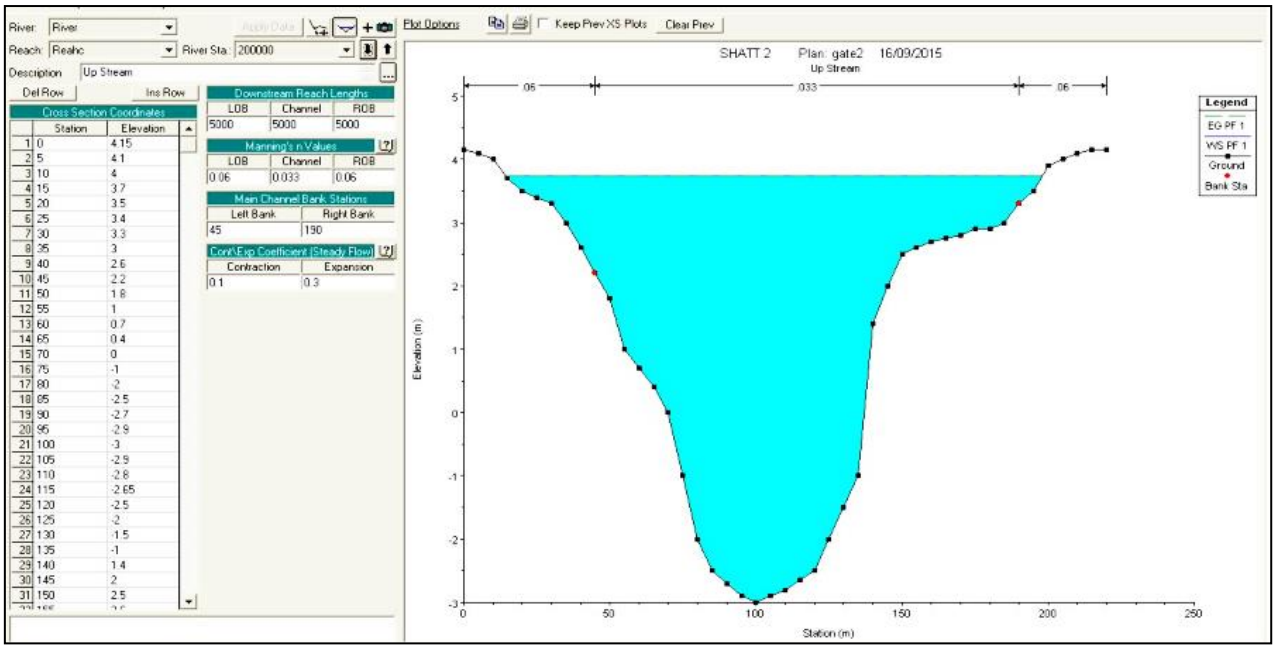

Figure 4. Cross-Profile of the river

3. Hydrodynamic Model

Unsteady or transient flow in rivers is simulated by two partial differential equations expressing the conservation of mass and momentum, known as the unsteady flow equations; they are often referred to as the Saint-Venant equations and are based upon the following assumptions (Chow 1959 [26]):

1. Flow is 1D; profundity and speed fluctuate just in the channel's longitudinal course. This infers speed is consistent and that the water surface is even over any area opposite to the longitudinal hub. Flow varies along the channel, meaning hydrostatic pressure prevails and vertical accelerations can be neglected.
2. The longitudinal hub of the channel is a straight line.
3. The base incline of the channel is little and the channel bed is fixed; the impact of scour and affidavit is insignificant.
4. The obstruction coefficient for consistent uniform violent stream is appropriate; connections, for example, Manning's condition, can be utilized to portray opposition impacts.
5. The liquid is incompressible and of consistent thickness all through the stream

The following derivation is for 1D equations in which the dependent variables are mean velocity (v) and average water depth (y) and the independent variables are longitudinal distance (x) and time (t).

The continuity equation may be written in term of velocity as:

$$\mathrm{A}\frac{\partial V}{\partial x}+V\frac{\partial \mathrm{A}}{\partial x}+\mathrm{B}\frac{\partial y}{\partial t}-q=0 \tag{6}$$

The resultant force on the element is equal to the sum of the pressure, gravitational forces and frictional forces, meaning:

$$\rho.g.\mathrm{A}\frac{\partial Z}{\partial_{\mathrm{X}}}\Delta \mathrm{X}-\rho.g.\mathrm{A}.S_f\Delta \mathrm{X}-.\rho.g.\mathrm{A}\frac{\partial y}{\partial x}\Delta \mathrm{X} \tag{7}$$

The total rate of momentum change is the sum of local and convective momentum changes, thus:

$$\rho.\Delta x\left(A\frac{\partial V}{\partial t}+V\frac{\partial A}{\partial t}\right)+\rho.V.\Delta x\left(V\frac{\partial A}{\partial x}+2A\frac{\partial V}{\partial x}\right) \tag{8}$$

The momentum equation becomes the following for lateral inflow:

$$\frac{\partial Q}{\partial t}+\frac{\partial}{\partial x}\left(\frac{Q^2}{\mathrm{A}}\right)+q.V_x=g.\mathrm{A}\left(S_o-S_f-\frac{\partial y}{\partial x}\right) \tag{9}$$

The momentum equation becomes the following for lateral outflow:

$$\frac{\partial Q}{\partial t}+\frac{\partial}{\partial x}\left(\frac{Q^2}{\mathrm{A}}\right)-q\frac{Q}{\mathrm{A}}=g.\mathrm{A}\left(S_o-S_f-\frac{\partial y}{\partial x}\right) \quad (10)$$

It is important to note that the contribution of lateral inflow and outflow to momentum change is generally very small and may be neglected. Variations of Equations 6 and 10 in conservation and non-conservation forms are used to define various 1D distributed routing models.

4. Method of Numerical Modelling

These conditions are too unpredictable to possibly be tackled through systematic strategies. It is conceivable, be that as it may, to discover surmised arrangements, which means stages and releases at a specific number of focuses in the time-space area in a way that fulfills the fundamental laws however much as could reasonably be expected. Discretisation is the way toward communicating general stream laws, composed for a consistent medium, as far as discrete qualities at a limited number of focuses in the stream field. Discretised stream laws would then be able to be numerically understood to outfit building arrangements. The subsidiaries are supplanted by isolated augmentation contrasts. Along these lines, the differential conditions (the laws portraying the continuum), are supplanted by logarithmic limited contrast connections. The manners by which subordinates are communicated by discrete capacities are called limited contrast plans.

In this method, the channel is divided into several reaches, usually having equal lengths of Δx. The ends of the reaches are called computational nodes or grid points. If the channel is divided into N reaches and the first node (upstream end) is numbered as 1, the last node (downstream end) will be N+1. The nodes at the upstream and downstream ends are called boundary nodes; those remaining are called interior nodes. Computations are performed at specific times. The difference between two consecutive times is called the computational time interval or computational time step.

The partial derivatives of the governing Equations 6 and 10 are replaced by the finite difference approximations, which then solve the resulting algebraic equations at each grid point. The velocity and depth of flow at all grid points is assumed to be known at time (t_o) - the objective is to determine their values at time ($t + \Delta t$). Initial values may be computed from initial conditions or from the previous time interval. It is typically necessary for the explicit finite difference scheme that the ratio of Δx and Δt satisfies an important criterion - stability. A scheme is said to be stable if an error introduced does not grow as the computation progresses in time; the scheme is said to be unstable if the error is amplified with time.

The relationships among the variables result from the equations of unsteady flow after the time and space partial derivatives of these equations have been replaced by the corresponding finite difference approximations. The finite difference equation then constitutes a system of nonlinear simultaneous algebraic equations, a characteristic requiring the use of an iterative solution procedure.

The mathematical model for solving the basic differential equations of gradually varied, unsteady 1D flow in the Euphrates River was applied and, using a computer, was used to solve the problem. The basic model has been calibrated and verified using field measurements of stage and discharge in the river; this was done through variation in the weighting factor, Manning roughness coefficient and time interval to accurately predict stage and discharge at any location along the river.

5. Results and Discussion

The application of a simulation model to natural channels allows for the determination of several physical and hydraulic properties of prototype systems. Some of these are readily available from direct field measurement while others must be approximated. Computational control parameters affect the accuracy, convergence and stability of numerical solutions. The primary considerations for numerical computations are the time increment (Δt), reach length (Δx), and weight factor (θ). The accuracy of initial conditions and the value of tolerance limits are also important.

Operation forms the model was used as a tool to adjust all assumptions of physical and hydraulic parameters through calibration. This process refines parameters and offers results nearest to the prototype. Concerning physical parameters, they are well defined, measurable and are less subject to adjustment than those for non-measured alternatives. Therefore, these parameters were reasonably assumed within an acceptable range.

5.1. Initial Conditions

Initial values are the most fundamental part of data for operating a model and inferring results. Initial values, represented by the depth (y) and discharge (Q) at time (j_{th}), may be measured directly from the field or obtained from the computation of a previous modelling process.

The initial water surface profile was adopted from backwater computations using steady-state conditions. Measurement of initial conditions requires the simultaneous measurements of depth and discharge at all points along the river. This method presents obvious difficulties and is often completely impractical at times. Arriving at the correct solution requires initial values to be reasonably accurate; otherwise, the initialisation error results in a much longer process. Computed water surface profiles for initial conditions in the Euphrates River are shown in Figures 5 and 6.

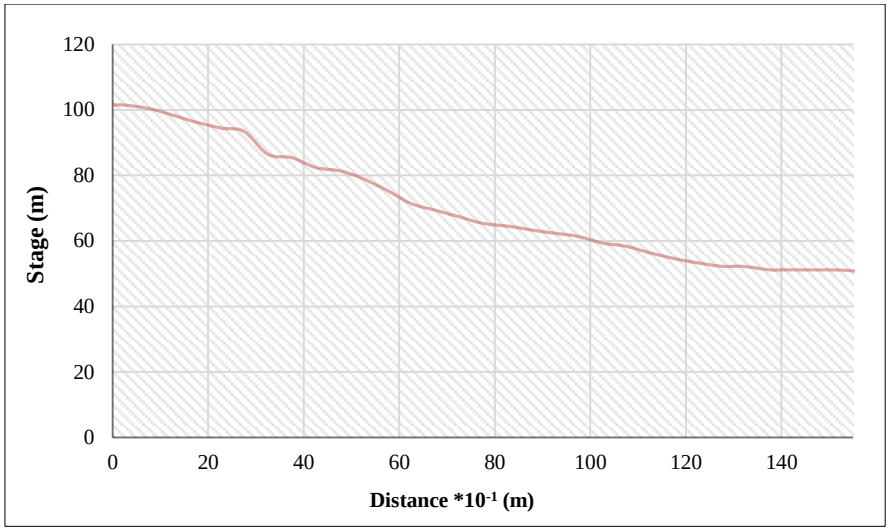

Figure 5. Stage Initial Condition for the Study Reach at 1/4/2017

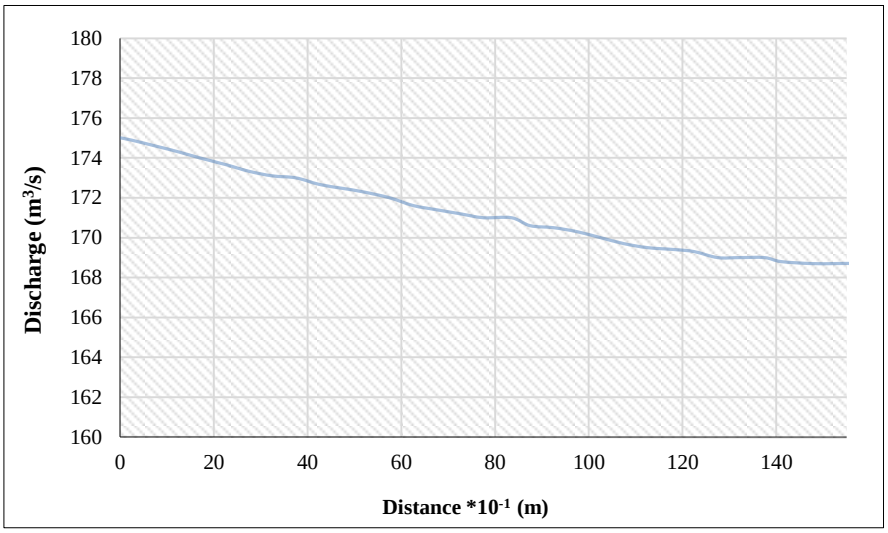

Figure 6. Discharge Initial Condition for the Study Reach at 1/4/2017

5.2. Boundary Conditions

Upstream boundary conditions consisted of discharge hydrograph (shown in Figure 7), for Station (2) at downstream site, were measured at daily intervals. The hydrograph was converted to tabulated values at 24-hour intervals while running the simulation. Linear interpolation between two adjacent values was used whenever model requirement discharge at shorter intervals. A stage hydrograph at station 16 was used as the downstream boundary condition for the Al-Hindiya Barrage at upstream sites as shown in Figure 8. All data was recorded between 1/4/2017 and 30/4/2017 and was divided into two sets, one for calibration purpose and another for verification.

5.3. Bed Channel Slope

River system always is illegal in its slope, so sections take adverse slope (ascent slope), when the flow proceeds to front head instead take descent slope. This case may interpret due to difference bed level of the reach, meaning it causes problems for the proper operation of the model. To solve this problem, adjustments must be made to all fluvial bed levels using a fit descent curve; this is done by considering a new bed level and computing depth in the cross-section area. Figure 9 shows bed levels before and after adjustment; a general agreement between them is evident.

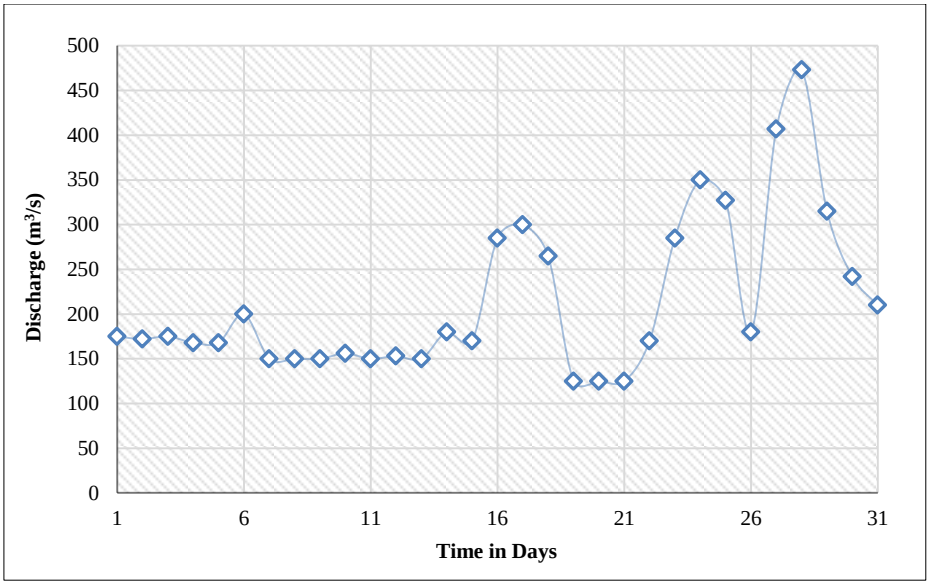

Figure 7. Discharge Hydrograph at Upstream Boundary Conditions

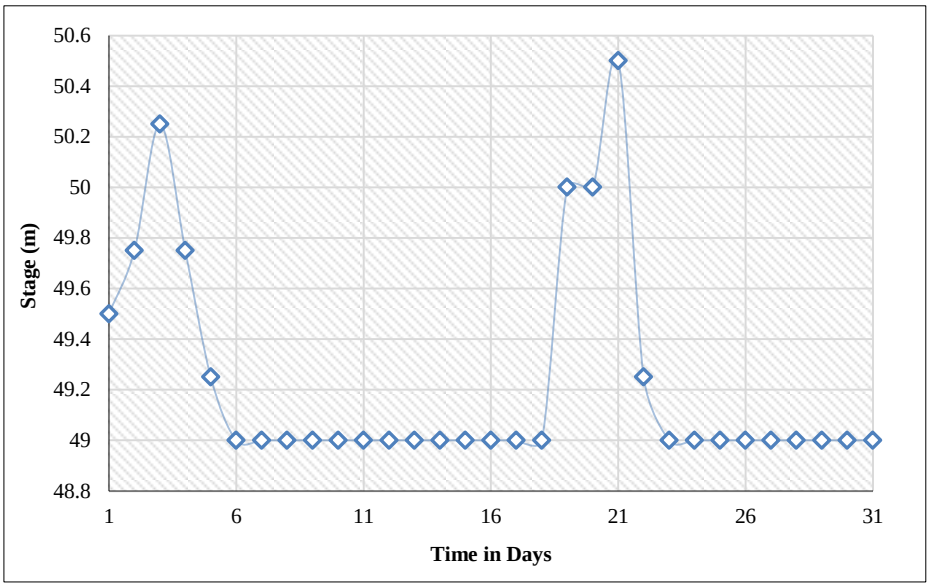

Figure 8. Stage Hydrograph at Downstream Boundary Conditions

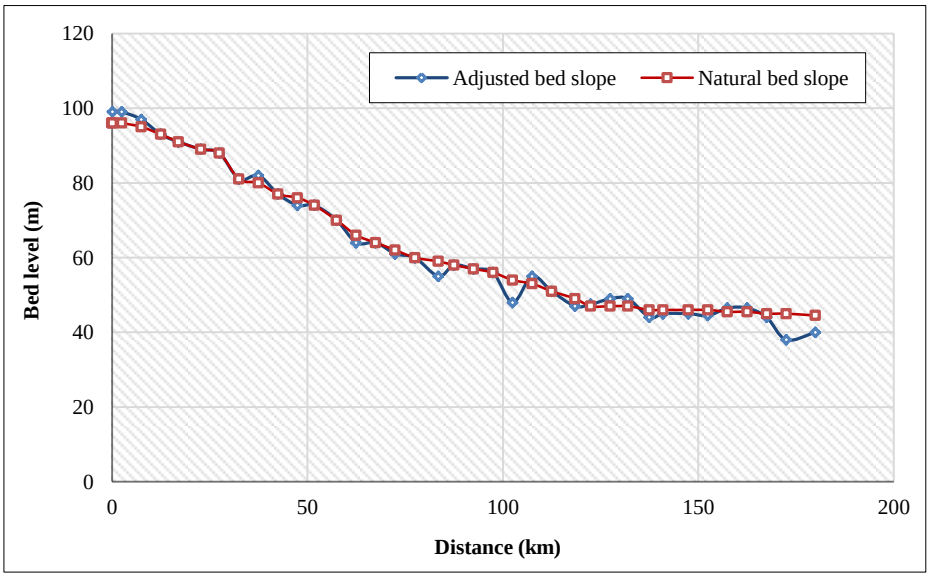

Figure 9. Comparison between Natural and Adjusted Bed Slope

5.4. Model Calibration

Model calibration is the process of adjusting the dimensions of simplified geometrical elements and the values of empirical coefficients to make a model's simulation as similar as possible to the natural event being studied. In the case of the Euphrates River simulation, proper calibration primarily involves n (the flow resistance coefficient), the appropriate value of time step Δt, and weighting factor θ. Since the calibration is also affected by the solution algorithm, which involves an iteration process, it is necessary to specify tolerance limits for the values at which the iteration process is terminated. The iteration is usually terminated if the change in stage and discharge values in two consecutive iterations is within ($\pm 1\%$ m) or (($\pm 1\%$ m^3/sec). Our calibration process used station (1) at the Al-Hindiya Barrage and station (2) at the end of the reach for comparison; the discharge hydrograph at station (1) was used as an upstream boundary condition for the simulation model.

5.4.1. Effect of the Manning Roughness Coefficient (n)

To study the effective of range varying Manning's roughness coefficient n on performed results a series of computation with specified values of $\Theta = 0.95, \Delta t = 24$ hours and without lateral outflow $q = 0\ m^3/sec/km$. In this computation, the assumed values of n range between 0.022 and 0.028. Results of the simulation model with these values were compared with the observed discharge and stage hydrographs measured at station (1) and station (2).

Table 2 shows the accuracy of results with each n value used; the root mean square error (RMSE) is used as an index of result accuracy with respect to stage and discharge. Figures 10 to 12 display the difference between observed and computed values for stage and discharge with different values of n. This difference between observed and computed values was substantial on 5/4/2017, 10/4/2017 and 15/4/2017.

The appropriate values of Manning's n appear to be in the range ($0.022 \leq n \leq 0.028$), which covers conditions encountered during the calibration period (1/3/2002 to 16/3/2002). However, a good agreement is obtained when n of 0.024, showing that n is an inclusive value that considers losses and not value strictly comparable to n in Manning's formula.

Table 2. Effect of Manning n on Computation of Water Elevation and Discharge in the Euphrates River

Section	Δt (hrs.)	Θ	n	Discharge (RMSE)	Stage (RMSE)
			0.022	0.013633	
1	24	0.95	0.024	0.014366	No observed data
			0.028	0.05084	
			0.022	0.01378	1265
2	24	0.95	0.024	0.01128	1131
			0.028	0.026233	1269

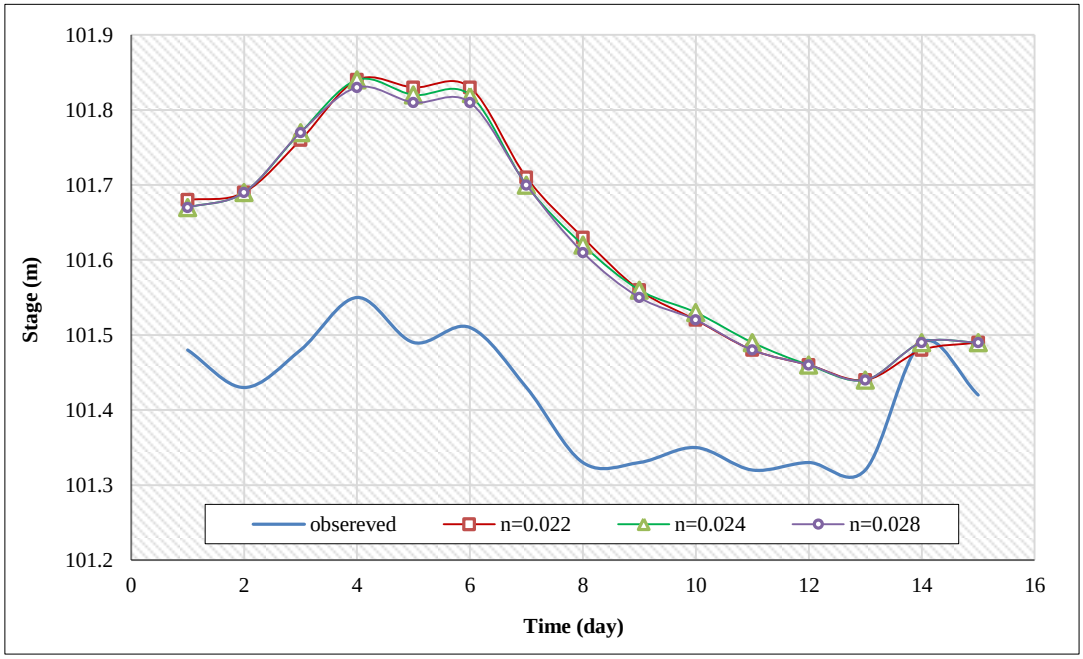

Figure 10. Comparison between Natural and Adjusted Bed Slope

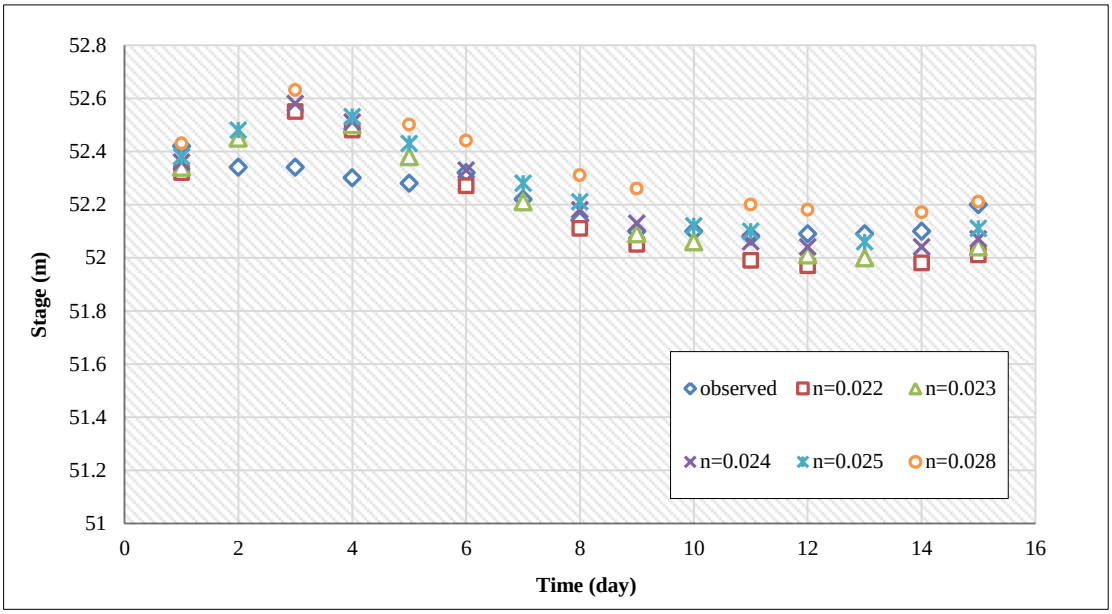

Figure 11. Observed and Computed Stage hydrograph at Station no. (2), with Different Manning's Roughness Coefficient n, ($\theta = 0.95, \Delta t = 24\ hrs$)

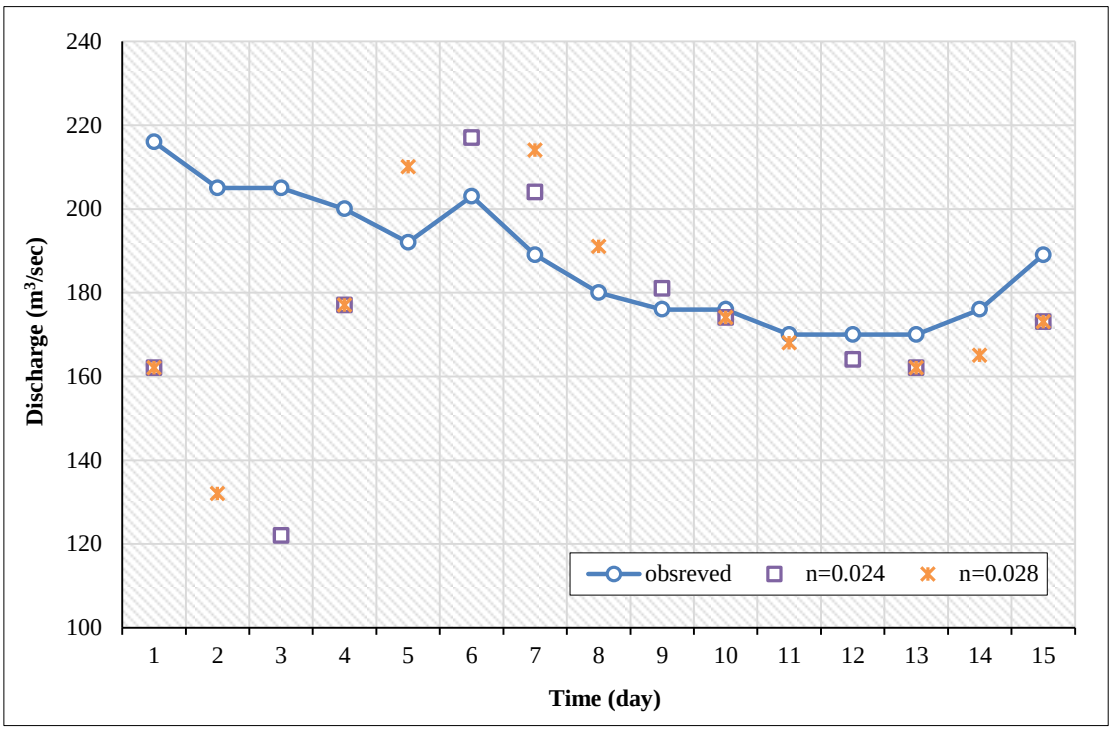

Figure 12. Observed and Computation Discharge Hydrograph at Station no. (2), with different Manning's Roughness Coefficient n, ($\theta = 0.95, \Delta t = 24\ hrs$)

5.4.2. Effect of Weighting Factor (θ)

The effects of the weighting factor (θ) on the stability, accuracy and convergence rate. The solution was evaluated using (θ) = 0.55, 0.75 and 0.95; the values of the other parameters were held constant (Δt = 24 hrs., q = 0, and n = 0.023). Comparisons between observed and computed hydrographs for stations (1) and (2) are shown in Figures 13 to 15. For both stations, (θ) = 0.95 produced hydrographs closer to observed values than both (θ) = 0.55 and (θ) = 0.75. Table 3 illustrates the convergence of the results obtained at both stations using RMSE as an index of accuracy between computed and observed data. Values of θ that give stable and accurate solutions appear to be in the range ($0.55 \leq (\theta) \leq 0.95$). However, reliable results were obtained with a weighting factor of 0.95.

Table 3. Effect of Weighting Factor Θ on Computation of Water Elevation and Discharge in the Euphrates River

Section	Δt (hrs.)	*n*	Θ	Stage (RMSE)	Discharge (RMSE)
			0.55	0.0168	
1	24	0.023	0.75	0.0142066	No observed data
			0.95	0.0125466	
			0.55	0.0146867	1451
2	24	0.023	0.75	0.012693	1226
			0.95	0.01132	1190

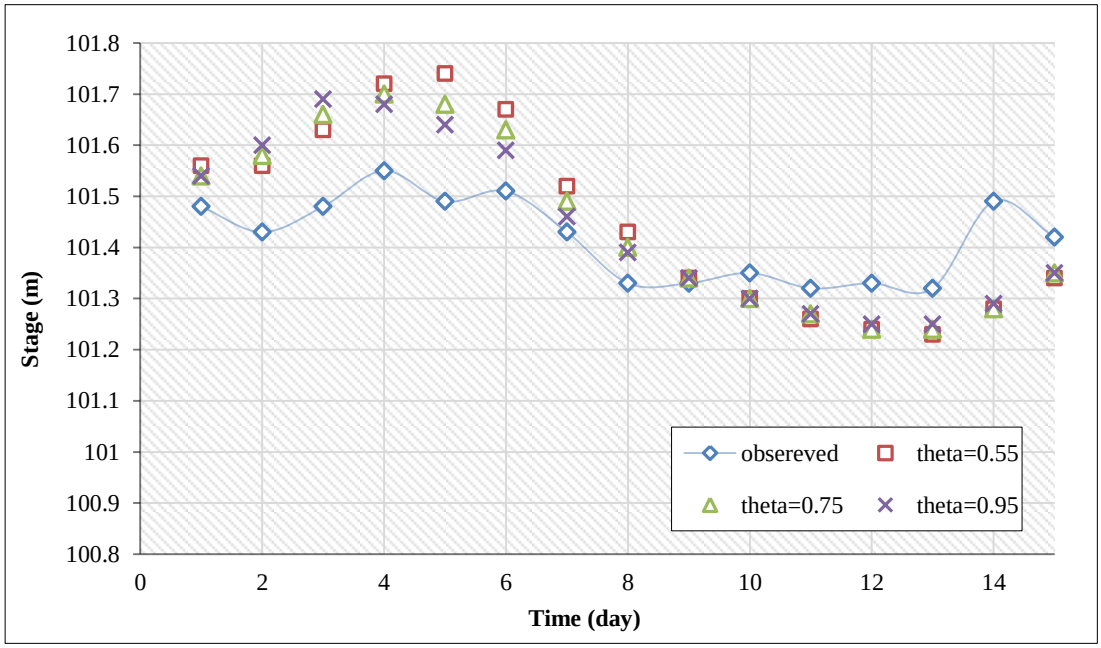

Figure 13. Observed and Computed Stage Hydrograph at Station no. (1), with different Weighting Factor Θ, ($n = 0.023, \Delta t = 24\ hrs$)

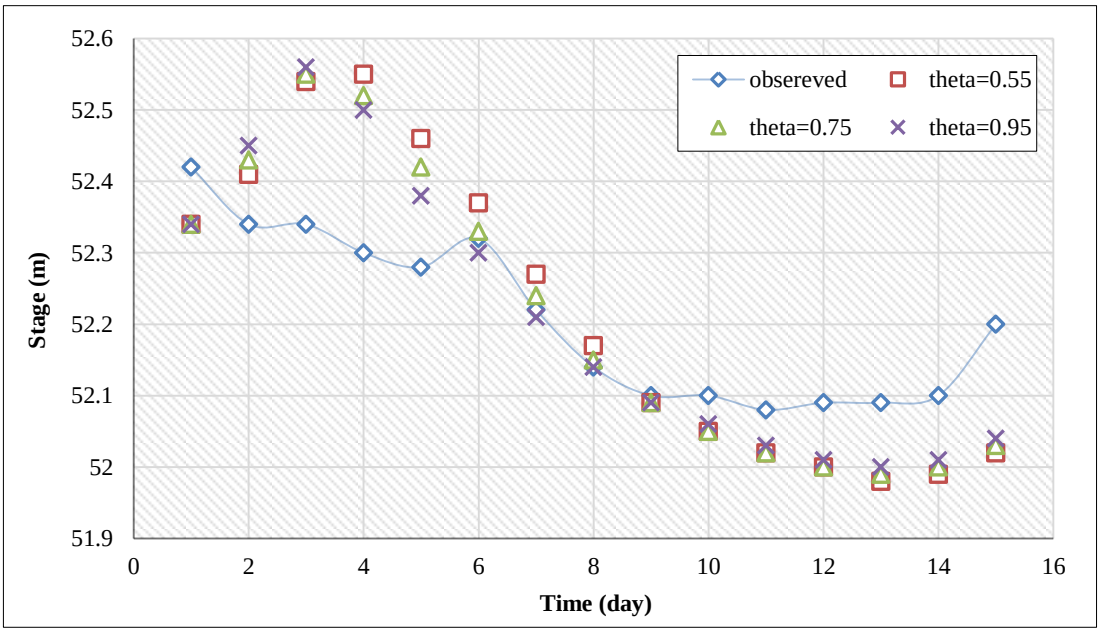

Figure 14. Observed and Computed Stage Hydrograph at Station no. (2), with different Weighting Factor Θ, ($n = 0.023, \Delta t = 24\ hrs$)

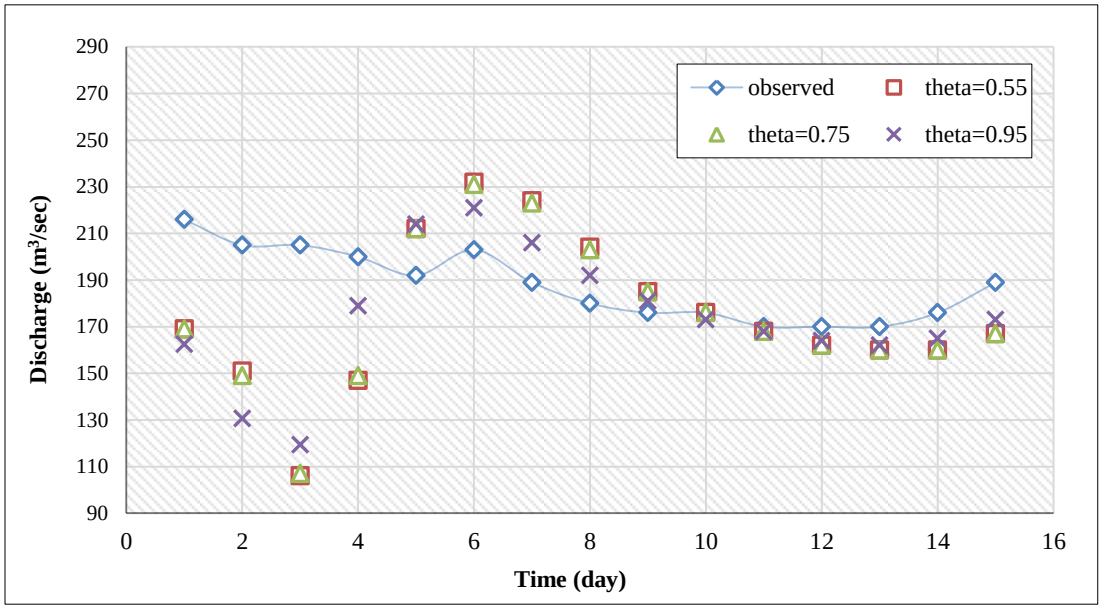

Figure 15. Observed and Computed Discharge Hydrograph at Station no. (2), with different Weighting Factor Θ, ($n = 0.023, \Delta t = 24\ hrs$)

5.4.3. Effect of Segment Length and Time Increment Δt

The last parameter in the calibration of flow simulation was the time increment Δt. Restrictions on the size of the time increment, imposed by explicit finite difference or the characteristics method, are explained by a necessary condition given by the following (Fread 1982 [27]).

$$\Delta t \leq \frac{\Delta X}{\left|V + \sqrt{gy}\right|} \tag{11}$$

Where: Δt = time increment (T); Δx = distance increment (segment length) (L); V = mean velocity (L/T); g = acceleration due to gravity (L/T^2); y = depth of flow (L)

The above relations are no longer applicable in implicit models; consequently, the only constraints are those imposed by the proper balance between the accuracy of the results and the cost of the computations. Unfortunately, segment length in natural channels depends on available data, which limits the selection of Δx.Therefore, for irregular distances between selected sections, it is necessary to select the smallest computed value of Δt for entire reaches. Increasing the time increment may limit the accuracy of simulation results. Three different computational time steps of 6, 12 and 24 hours were used with a fixed value of Θ = 0.95 and Manning coefficient (n = 0.023).

The resulting stage hydrographs for station (1) are shown in Figure 13. Changing the value of Δt does not produce significant differences in stage hydrographs, as demonstrated by the RMSE of water surface elevation with values of 0.014533, 0.013553 and 0.0125466 for Δt of 6, 12 and 24 hours respectively—this is shown in Table 4. Relatively large RMSEs for the 6 and 12-hour time increments may be due in part to linear interpolation of observed hydrographs, which was measured at 24-hour intervals. Figures 14 and 15 from station (2) provide closer results to observed values for time step Δt = 24 hrs.

The data recorded at a time increment of 24 hours was proposed to provide accurate observations and enhanced computation costs. However, the flow in the Euphrates River was gradually varied due to slight changes each day. Therefore, it was possible to use a time step of 12 hours instead. Comparisons between explicit and implicit solutions revealed that the explicit method required a relatively restrictive relationship between Δx and Δt.

Table 4. Effect of Time Increment Δt on Computation of Water Elevation and Discharge in the Euphrates River

Section	Θ	n	Δt (hrs.)	Stage (RMSE)	Discharge (RMSE)
1	0.95	0.023	6	0.014533	No observed data
			12	0.013553	
			24	0.0125466	
2	0.95	0.023	6	0.0146	1487
			12	0.01287	1330
			24	0.01132	1190

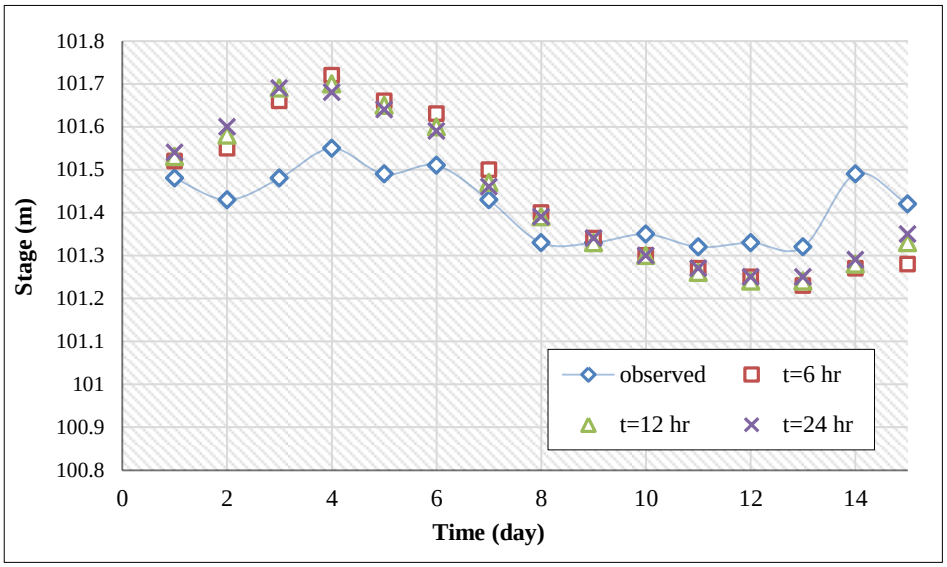

Figure 13. Observed and Computed Stage Hydrograph at Station no. (1), with different time increment Δt, (n = 0.023, θ = 0.95)

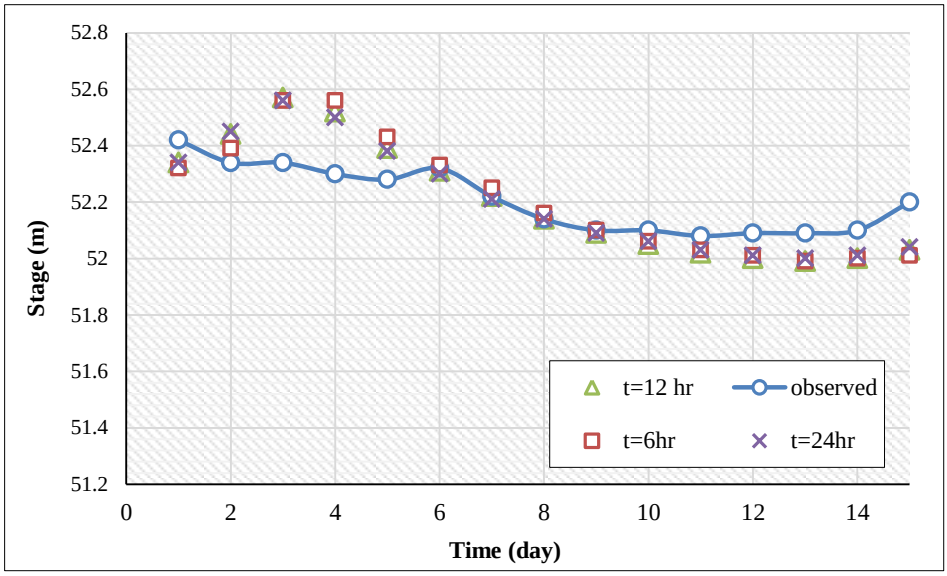

Figure 14. Observed and Computed Stage Hydrograph at Station no. (2), with different time increment Δt, (n = 0.023, θ =0.95)

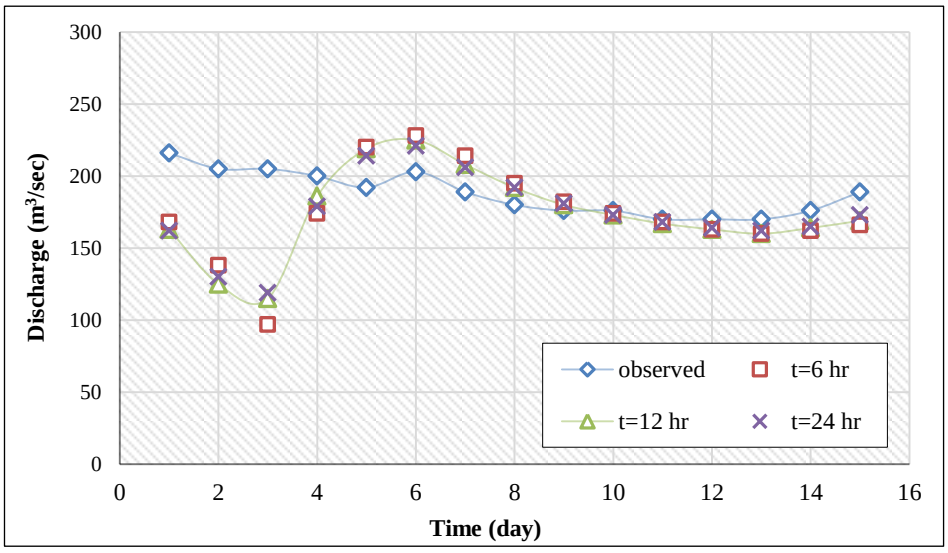

Figure 15. Observed and Computed Discharge Hydrograph at Station no. (2), with different time increment Δt, (n = 0.023, θ = 0.95)

5.5. Verification of Hydrodynamic Model

The real test of any simulation model is its application to an independent set of conditions using parameters derived from the calibration runs. A model's validity is defined by its applicability to situations other than those used during calibration. For this purpose, the data recorder from 16/4/2017 to 31/4/2017 was used. The discharge hydrograph at station (1) was held as an upstream boundary condition and used to predict the stage hydrograph for stations (1) and (2). The verification performed by comparing predicted and observed hydrographs is shown in Figures 16 and 17.

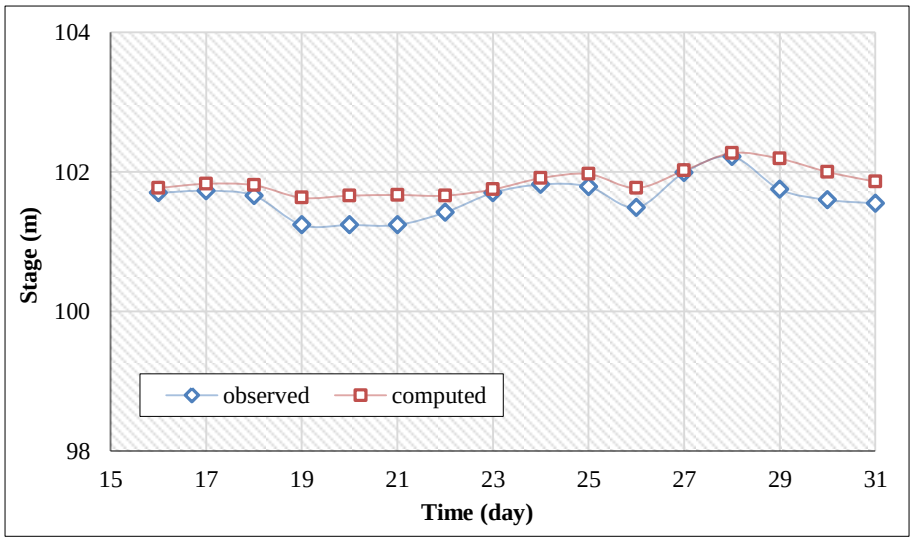

Figure 16. Model Verification: Observed and Predicted Euphrates River hydrograph at Station (1)

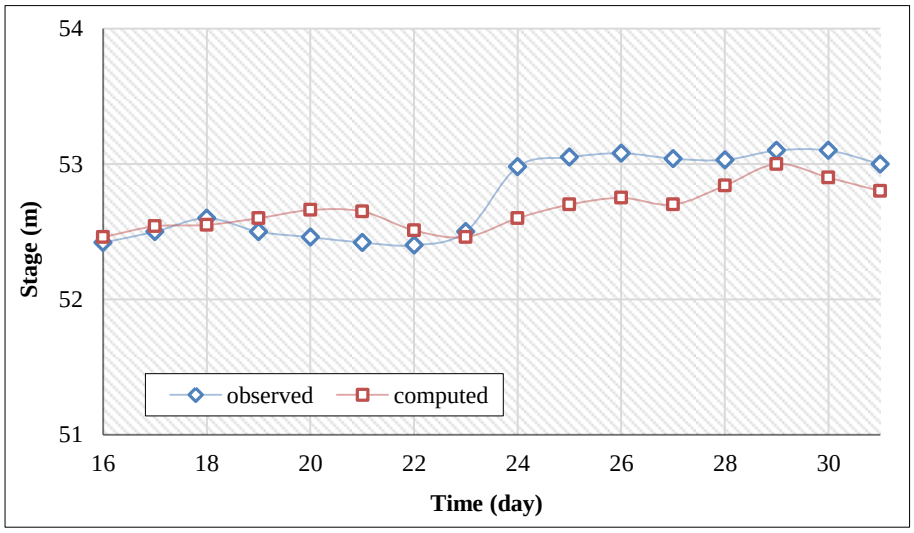

Figure 17. Model Verification: Observed and Predicted Euphrates River hydrograph at Station (2)

6. Conclusions

Results of calibration and verification demonstrate the following:

- The values of weighting factor Θ that give stable and accurate solutions appear to be in the range ($0.55 \leq \Theta \leq 0.95$). However, reliable results are best obtained using a factor of 0.95;
- The data recorded at a time increment of 24 hours was proposed to provide accurate observations and enhanced computation costs. However, the flow in the Euphrates River was gradually varied due to slight changes each day, so it was possible to use a time step of 12 hours instead;
- Acceptable values of Manning's n appear to be in the range ($0.022 \leq n \leq 0.028$), which covers conditions encountered during the calibration period (1/4/2017 to 16/4/2017). However, good agreement is obtained when an n of 0.024 is used, showing that n is an inclusive value that considers losses and not value strictly comparable to n in Manning's formula;

- Verification of the hydrodynamic model show that very close results are obtained using ($\Delta t = 24\,hrs$), ($\Theta = 0.95$) and (n = 0.024);
- Comparisons between explicit and implicit solutions revealed that the explicit method required a relatively restrictive relationship between Δx and Δt.

7. Conflicts of Interest

The authors declare no conflict of interest.

8. References

[1] Jacob, Xavier K., Deepak Singh Bisht, Chandranath Chatterjee, and Narendra Singh Raghuwanshi. "Hydrodynamic Modeling for Flood Hazard Assessment in a Data Scarce Region: a Case Study of Bharathapuzha River Basin." Environmental Modeling & Assessment 25, no. 1 (April 12, 2019): 97–114. doi:10.1007/s10666-019-09664-y.

[2] Buček, Daniel, Martin Orfánus, and Peter Dušička. "Assessment of River Bed Evolution with the Aid of 2D Hydrodynamic Model with Integrated Sediment Transport Modeling Capabilities." Pollack Periodica 14, no. 1 (April 2019): 129–138. doi:10.1556/606.2019.14.1.13.

[3] Glubt, Sarah Van, Scott Wells, and Chris Berger. "Hydrodynamic and Water Quality Modeling of the Chehalis River in Washington." World Environmental and Water Resources Congress 2017 (May 18, 2017). doi:10.1061/9780784480601.019.

[4] Sitek, M. A., S. A. Lottes, and C. Bojanowski. "Computational Assessment of Hydrodynamic Loads on Rockeries for River Bank Protection" (May 1, 2019). doi:10.2172/1523372.

[5] Brown, Gary, Jennifer McAlpin, Kimberley Pevey, Phu Luong, Cherie Price, and Barbara Kleiss. "Mississippi River Hydrodynamic and Delta Management Study : Delta Management Modeling : AdH/SEDLIB Multi-Dimensional Model Validation and Scenario Analysis Report" (March 29, 2019). doi:10.21079/11681/32446.

[6] Chen, Wei-Bo, and Wen-Cheng Liu. "Modeling the Influence of River Cross-Section Data on a River Stage Using a Two-Dimensional/Three-Dimensional Hydrodynamic Model." Water 9, no. 3 (March 10, 2017): 203. doi:10.3390/w9030203.

[7] Pramanik, Niranjan, Rabindra Kumar Panda, and Dhrubajyoti Sen. "One Dimensional Hydrodynamic Modeling of River Flow Using DEM Extracted River Cross-Sections." Water Resources Management 24, no. 5 (July 14, 2009): 835–852. doi:10.1007/s11269-009-9474-6.

[8] Shailesh Kumar Singh, "Analysis of uncertainties in digital elevation models in flood (hydraulic) modeling". Masters Thesis, International Institute of Remote Sensing, Dehradun, India. (2005). Online available: https://hindi.iirs.gov.in/iirs/sites/default/files/StudentThesis/shailesh_thesis2004_0.pdf (accessed on: 25 March 2020).

[9] Vijay, Ritesh, Aabha Sargoankar, and Apurba Gupta. "Hydrodynamic Simulation of River Yamuna for Riverbed Assessment: A Case Study of Delhi Region." Environmental Monitoring and Assessment 130, no. 1–3 (November 28, 2006): 381–387. doi:10.1007/s10661-006-9405-4.

[10] Wang, Jia-Song, Han-Gen Ni, and You-Sheng He. "Finite-difference TVD scheme for computation of dam-break problems." Journal of Hydraulic Engineering 126, no. 4 (2000): 253-262. doi:10.1061/(asce)0733-9429(2000)126:4(253)

[11] Gottardi, G., and M. Venutelli. "Central Scheme for Two-Dimensional Dam-Break Flow Simulation." Advances in Water Resources 27, no. 3 (March 2004): 259–268. doi:10.1016/j.advwatres.2003.12.006.

[12] Meng, Jian, Zhi-xian Cao, and Paul A. Carling. "Pointwise and Upwind Discretizations of Source Terms in Open-Channel Flood Routing." Journal of Hydrodynamics 18, no. 4 (August 2006): 379–386. doi:10.1016/s1001-6058(06)60108-x.

[13] Dutta, Dushmanta, Srikantha Herath, and Katumi Musiake. "Flood inundation simulation in a river basin using a physically based distributed hydrologic model." Hydrological Processes 14, no. 3 (2000): 497-519. doi:10.1002/(SICI)10991085(20000228)14:3<497::AID-HYP951>3.0.CO;2-U.

[14] Renyi, Liu, and Liu Nan. "Flood Area and Damage Estimation in Zhejiang, China." Journal of Environmental Management 66, no. 1 (September 2002): 1–8. doi:10.1006/jema.2002.0544.

[15] Merwade, Venkatesh, Aaron Cook, and Julie Coonrod. "GIS Techniques for Creating River Terrain Models for Hydrodynamic Modeling and Flood Inundation Mapping." Environmental Modelling & Software 23, no. 10–11 (October 2008): 1300–1311. doi:10.1016/j.envsoft.2008.03.005.

[16] Zhu, Fangfang, Wenrui Huang, Yi Cai, Fei Teng, Beibei Wang, and Qi Zhou. "Development of a River Hydrodynamic Model for Studying Surface-Ground Water Interactions Affected by Climate Change in Heihe River, China." Journal of Coastal Research 68 (November 2014): 129–135. doi:10.2112/si68-017.1.

[17] Langevin, Christian, Eric Swain, and Melinda Wolfert. “Simulation of Integrated Surface-Water/ground-Water Flow and Salinity for a Coastal Wetland and Adjacent Estuary.” Journal of Hydrology 314, no. 1–4 (November 2005): 212–234. doi:10.1016/j.jhydrol.2005.04.015.

[18] Akiyama, Tomohiro, Akiko Sakai, Yusuke Yamazaki, Genxu Wang, Koji Fujita, Masayoshi Nakawo, Jumpei Kubota, and Yuki Konagaya. "Surfacewater-groundwater interaction in the Heihe River basin, Northwestern China." Bulletin of Glaciological Research 24 (2007): 87.

[19] Candela, Lucila, Wolf von Igel, F. Javier Elorza, and Giuseppe Aronica. “Impact Assessment of Combined Climate and Management Scenarios on Groundwater Resources and Associated Wetland (Majorca, Spain).” Journal of Hydrology 376, no. 3–4 (October 2009): 510–527. doi:10.1016/j.jhydrol.2009.07.057.

[20] Scibek, Jacek, Diana M. Allen, Alex J. Cannon, and Paul H. Whitfield. “Groundwater–surface Water Interaction under Scenarios of Climate Change Using a High-Resolution Transient Groundwater Model.” Journal of Hydrology 333, no. 2–4 (February 2007): 165–181. doi:10.1016/j.jhydrol.2006.08.005.

[21] Kafle, Mukesh Raj, and Narendra Man Shakya. “Two-Dimensional Hydrodynamic Modelling of Koshi River and Prediction of Inundation Parameters.” Hydrology: Current Research 09, no. 02 (2018). doi:10.4172/2157-7587.1000298.

[22] Neal, Jeffrey, Ignacio Villanueva, Nigel Wright, Thomas Willis, Timothy Fewtrell, and Paul Bates. “How Much Physical Complexity Is Needed to Model Flood Inundation?” Hydrological Processes 26, no. 15 (November 18, 2011): 2264–2282. doi:10.1002/hyp.8339.

[23] De Almeida, Gustavo A. M., and Paul Bates. “Applicability of the Local Inertial Approximation of the Shallow Water Equations to Flood Modeling.” Water Resources Research 49, no. 8 (August 2013): 4833–4844. doi:10.1002/wrcr.20366.

[24] Álvarez, Manuel, Jerónimo Puertas, Enrique Peña, and María Bermúdez. "Two-dimensional dam-break flood analysis in data-scarce regions: The case study of Chipembe dam, Mozambique." Water 9, no. 6 (2017): 432. 432. doi.org/10.3390/w9060432.

[25] Bermúdez, María, Jeffrey C. Neal, Paul D. Bates, Gemma Coxon, Jim E. Freer, Luis Cea, and Jeronimo Puertas. “Quantifying Local Rainfall Dynamics and Uncertain Boundary Conditions into a Nested Regional-Local Flood Modeling System.” Water Resources Research 53, no. 4 (April 2017): 2770–2785. doi:10.1002/2016wr019903.

[26] Chow, V. T. "Open channel hydraulics. MacGraw-Hill Book Co." Inc., New York, NY (1959): 206.

[27] Fread, D.L. "Channel Routing" Hydrologic Research Lab, National Weather Service, Silver Spring, Maryland, (1982).